ORIGINAL ARTICLE

Eberhard P. Scholz · Edgar Zitron ·
Claudia Kiesecker · Sonja Lück · Dierk Thomas ·
Sven Kathöfer · Volker A. W. Kreye · Hugo A. Katus ·
Johann Kiehn · Wolfgang Schoels · Christoph A. Karle

Inhibition of cardiac HERG channels by grapefruit flavonoid naringenin: implications for the influence of dietary compounds on cardiac repolarisation

Abstract Flavonoids are naturally occurring food ingredients that have been associated with reduced cardiovascular mortality in epidemiological studies. In a previous study, we demonstrated for the first time that flavonoids are inhibitors of cardiac human *ether-à-go-go*-related gene (HERG) channels. Furthermore, we observed that grapefruit juice induced mild QTc prolongation in healthy subjects. HERG blockade by grapefruit flavonoid naringenin is most likely to be the mechanism underlying this effect. Therefore, the electrophysiological properties of HERG blockade by naringenin were analysed in detail. HERG potassium currents expressed in *Xenopus* oocytes were measured with a two-microelectrode voltage clamp. Naringenin blocked HERG potassium channels with an IC_{50} value of 102.6 µM in *Xenopus* oocytes. The onset of blockade was fast. The effect was completely reversible upon wash-out. Naringenin binding to HERG required aromatic residue F656 in the putative pore binding site. Channels were blocked in the open and inactivated states but not in the closed states. Naringenin did not affect HERG current activation. However, the half maximal inactivation voltage was shifted by 14.9 mV towards more negative potentials and current inactivation at negative potentials was accelerated. No frequency dependence of blockade was observed. Naringenin inhibits HERG channels with pharmacological characteristics similar to those of well-known HERG antagonists. From a clinical point of view, this effect could have both proarrhythmic and anti-arrhythmic consequences. This may have important implications for phytotherapy and for dietary recommendations for cardiologic patients. Therefore, electrophysiological effects of flavonoids deserve further investigation.

Keywords Flavonoids · Grapefruit · Naringenin · HERG channel · Molecular electrophysiology · Potassium channels · Pharmacology · Arrhythmia

E. Scholz and E. Zitron contributed equally to this work

E. P. Scholz · E. Zitron (✉) · C. Kiesecker · S. Lück ·
D. Thomas · S. Kathöfer · H. A. Katus · J. Kiehn ·
W. Schoels · C. A. Karle
Department of Cardiology,
Medical University Hospital Heidelberg,
Im Neuenheimer Feld 410,
69120 Heidelberg, Germany
e-mail: e_zitron@yahoo.de
Tel.: +49-6221-5638992
Fax: +49-6221-565357

V. A. W. Kreye
Department of Physiology and Pathophysiology,
Medical University Hospital Heidelberg,
Im Neuenheimer Feld 410,
69120 Heidelberg, Germany

Introduction

Flavonoids represent a group of over 4,000 structurally related phenylchromones and are found in fruits, vegetables, nuts, herbs, spices, tea and wine (Middleton et al. 2000). Structurally similar to tocopherols, flavonoids exhibit strong antioxidant properties, act as enzyme inhibitors and show anti-inflammatory, antithrombotic, antiviral and anticarcinogenic potency.

In the context of the "French Paradox" and the "Mediterranean Diet", flavonoids are thought to play a major role in the prevention of coronary heart disease (CHD) and reduction of cardiovascular mortality (Renaud and de Lorgeril 1992; de Lorgeril 1998). As a consequence, their beneficial effects as dietary compounds have been examined in epidemiological studies. An inverse association between dietary intake of flavonoids and coronary heart disease was found by numerous groups (Knekt et al. 1996; Hertog et al. 1993; Geleijnse et al. 2002; Yochum et al. 1999; Rimm et al. 1996). Several properties of flavonoids provide mechanisms that may explain those beneficial effects, such as antithrombotic activity, antioxidant potential or inhibition of low-density lipoprotein (LDL) oxidation (Mukamal et al. 2002). However, it is an interesting finding that some of the studies reveal a greater

reduction in coronary mortality than CHD prevalence (Hertog et al. 1993; Geleijnse et al. 2002; Rimm et al. 1996; Mukamal et al. 2002). As arrhythmias induced by coronary events (i.e. myocardial infarction) are the main cause of death in CHD patients, this correlation may point to as yet unknown antiarrhythmic effects of flavonoids.

The human *ether-à-go-go*-related gene (HERG) encodes the α-subunit of I_{Kr}, which conducts one of the most important repolarising currents (Curran et al. 1995). HERG is the main molecular target of class III antiarrhythmic drugs and it is affected by several noncardiac drugs with HERG-mediated proarrhythmic potential (Redfern et al. 2003). In a previous study, we screened a broad spectrum of structurally different dietary flavonoids for their affinity to HERG channels (Zitron et al. 2005). Out of 21 compounds tested, 10 caused a significant blockade of HERG channels. The flavonoid with the highest potency was naringenin, the principal flavonoid found in grapefruits. Naringenin (Fig. 1) is abundant in grapefruit juice and reaches plasma concentrations in the micromolar range due to its good bioavailability. As a consequence, we were able to demonstrate that freshly squeezed grapefruit juice is suitable for inducing a mild QTc prolongation in healthy subjects, thus showing for the first time a direct effect of dietary compounds on cardiac electrophysiology in vivo. This effect is most likely to be due to fractional HERG channel blockade by naringenin.

In this study, we examine in detail the electrophysiological properties of HERG channel blockade by naringenin. We demonstrate that naringenin shares many properties of conventional HERG antagonists that may be associated with both proarrhythmic and antiarrhythmic activity in vivo.

Materials and methods

Solutions and drug administration Two-microelectrode voltage clamp measurements of *Xenopus* oocytes were performed in a low K^+ solution (containing in mM: KCl 5, NaCl 100, $CaCl_2$ 1.5, $MgCl_2$ 2 and HEPES 10, pH adjusted to 7.4). Current and voltage electrodes were filled with 3 M KCl solution. Naringenin was purchased from
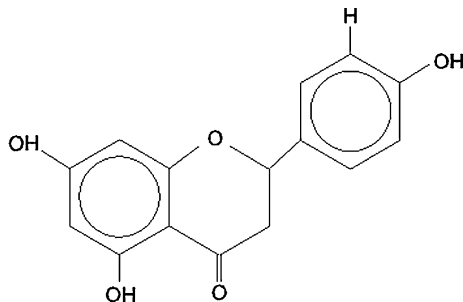
Sigma (Deisenhofen, Germany). For stock solutions, naringenin was dissolved in DMSO to a concentration of 10^{-1} M and stored at +4°C. On the day of the experiments, flavonoid stocks were diluted with bath solution to lower concentrations. The maximum concentration of DMSO (0.1% v/v) in the bath had no effect on the measured currents. All measurements were carried out at room temperature (20°C). The bath chamber volume was approximately 150 μl. After solution switch, it took approximately 4 s for the new solution to reach the bath (tubing length of about 37 cm). At a flow rate of 1 ml/min, the solution in the bath was totally exchanged within 9 s. In general, recording began 30 s after solution switch. All measurements were performed under steady-state conditions at least 2 min after total solution exchange.

Electrophysiology and data analysis The two-microelectrode voltage clamp configuration was used to record currents from *Xenopus laevis* oocytes. Microelectrodes had tip resistances ranging from 1 to 5 MΩ. Data were low-pass filtered at 1 to 2 kHz (−3 dB, four-pole Bessel filter) before digitalisation at 5–10 kHz. Recordings were performed using a commercially available amplifier (Warner OC-725A; Warner Instruments, Hamden, CT, USA) and pCLAMP software (Axon Instruments, Foster City, CA, USA) for data acquisition and analysis. No leak subtraction was performed during the experiments. Concentration–response curves were fitted with the Hill equation: $I/I_0 = I_0 / \left(1 + X/IC_{50}\right)^{n_H}$, with I/I_0 being the relative current, I_0 the unblocked current amplitude, X the flavonoid concentration, IC_{50} the dose for half maximal blockade and n_H the Hill coefficient. Statistical data are expressed as mean ± standard error with *n* representing the number of experiments performed. Statistical significance was evaluated using paired and unpaired Student's *t* tests.

Expression of HERG wild type and mutant channels in Xenopus oocytes The HERG clone (GenBank accession no. hsu04270) was generously donated by M.T. Keating (Salt Lake City, Utah, USA). Generation of mutated HERG channels HERG Y652A and HERG F656A was described previously (Scholz et al. 2003). HERG complementary RNA was prepared from HERG cDNA in the pSP64 vector with the mMESSAGE mMACHINE in vitro transcription kit (Ambion, Austin, TX, USA) by use of SP6 Polymerase after linearisation with EcoRI (Roche, Mannheim, Germany). Injection of RNA (50–500 ng/μl) into stage V and VI defolliculated oocytes was performed by using a Nanoject automatic injector (Drummond, Broomall, PA, USA). The volume of injected cRNA solution was 46 nl per oocyte, and measurements were performed 2–7 days after injection. The investigation conforms with the *Guide for the Care and Use of Laboratory Animals* published by the US National Institutes of Health (NIH publication No. 85-23, revised 1996).
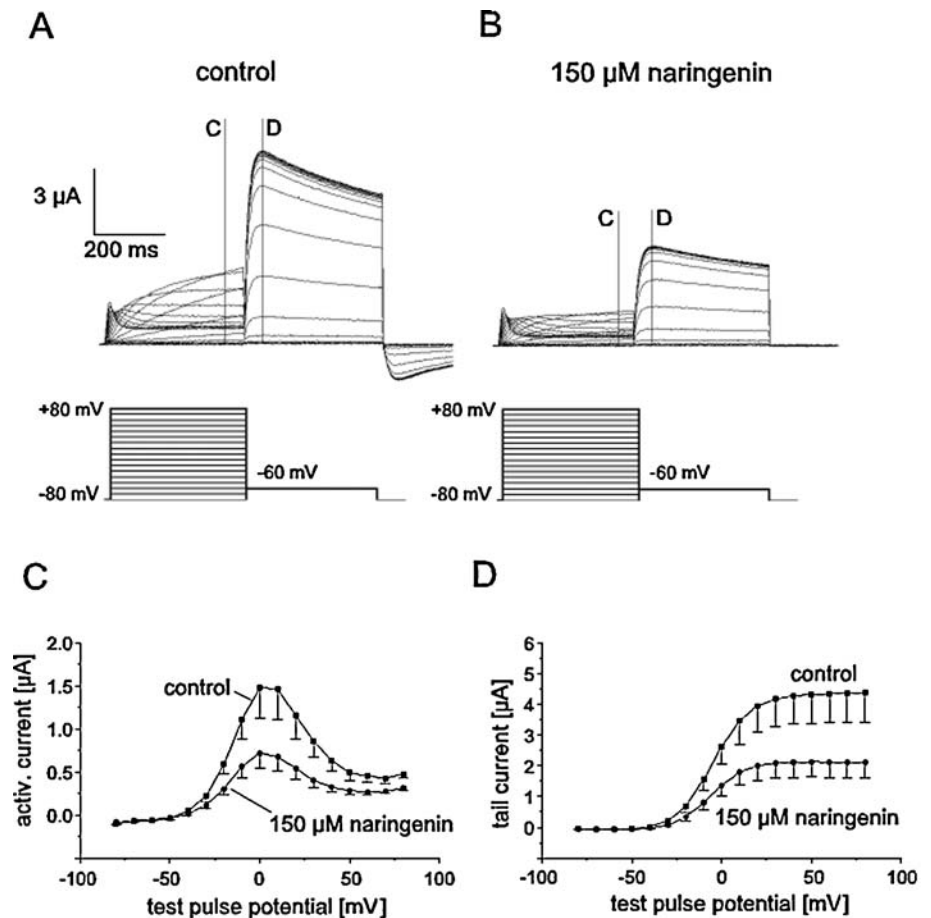

Fig. 1 Chemical structure of naringenin

Results

Grapefruit flavonoid naringenin inhibits HERG potassium currents

Human *ether-à-go-go*-related gene channels were expressed heterologously in *Xenopus* oocytes. A two-step voltage protocol was used to elicit typical HERG currents: from a holding potential of −80 mV, test pulses from −80 to +80 mV in 10 mV-increments (400 ms) were applied, which triggered activating currents. Each pulse was followed by a constant return pulse to −60 mV (400 ms) to evoke outward tail currents. After having obtained control measurements (Fig. 2a), naringenin (150 μM) was washed into the bath for 10 min and measurements were repeated (Fig. 2b). Naringenin markedly inhibited both HERG activating and tail currents.

Current–voltage relations of activating currents at the end of the first test pulse exhibited the typical bell-shaped appearance (Fig. 2c). Activating current amplitudes at 0 mV were reduced to 47.9±3.1% of control values (*n*=8). In Fig. 2d, peak tail current amplitudes are plotted as a function of the preceding test pulse potential showing a reduction to 49.2±3.9% of respective control values after a test pulse to 30 mV (*n*=8).

Concentration dependence of blockade

Human *ether-à-go-go*-related gene tail current amplitudes were measured to quantify relative blockade. From a holding potential of −80 mV, test pulses to +30 mV (400 ms) and return pulses to −60 mV (400 ms) were applied to elicit tail currents. Naringenin was washed into the bath at increasing concentrations (1, 10, 100, 300 and 1,000 μM). The resulting concentration–response curve (Fig. 3) was fitted with the Hill equation and yielded an IC_{50} value of 102.6 μM (*n*=4–5; n_H=1.72).

Significance of residues Y652 and F656 for binding of naringenin to HERG channels

Numerous HERG blocking agents access a common binding site within the putative HERG channel pore cavity with the main molecular determinants Tyr-652 and Phe-656 (Mitcheson et al. 2000). We used Y652A and F656A mutant HERG channels to investigate the significance of this drug receptor for the binding of naringenin. As heterologous expression of these mutant channels is lower than that of wild type channels, we did not use the outward tail current protocol underlying Figs. 2, 3. Instead, we
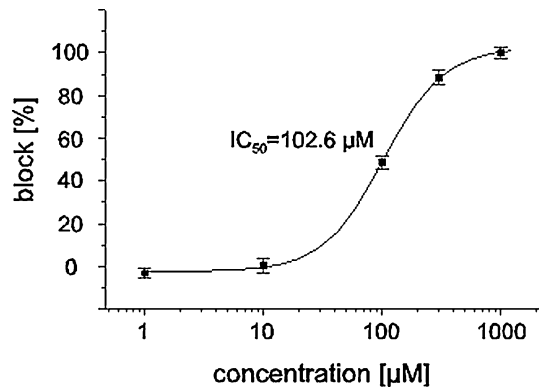

Fig. 2 Inhibition of human *ether-à-go-go*-related gene (HERG) currents by naringenin. HERG currents heterologously expressed in *Xenopus* oocytes **a** under control conditions and **b** after inhibition by 150 μM naringenin. **c**, **d** Mean data of *n*=6 experiments. **c** Current–voltage relations of the activating currents at the end of the first test pulse. **d** Peak tail currents plotted as a function of the preceding test pulse potential. Protocol: holding potential −80 mV, first pulse −80 mV to +80 mV (400 ms) in 10-mV increments, return pulse constantly −60 mV (400 ms)

Fig. 3 Concentration–effect relations. Concentration–response curves were fitted with the Hill equation: the IC_{50} was 102.6 µM (n=5–6)

fusion with the bath solution, that we have also observed in previous studies (Kiesecker et al. 2004). This phenomenon has also been reported by other electrophysiologists and is generally attributed to unspecific properties of the expression system (Witchel et al. 2002). During the observation time underlying the study experiments, we found an increase to 132.2±10.5% (n=6) of the initial values, which is also shown in Fig. 4d for comparison (left columns indicated as "control"). Naringenin applied at a concentration of 1 mM caused a profound inhibition of HERG wild type currents (second column from the left). The inhibitory effect of naringenin was markedly attenuated in HERG F656A channels (P=7.1*10^{-4}, n=6), but not significantly altered in HERG Y652A channels (P>0.05; n=5).

chose a modified voltage protocol that elicits large inward tail currents to minimise recording errors and allow reliable data analysis. From a holding potential of −80 mV, a depolaring test pulse to +30 mV (400 ms) triggered activating currents and a subsequent repolarising pulse to −120 mV (400 ms) evoked inward tail currents (Fig. 4a–c). Measurements of HERG wild type channels under control conditions and after exposure to 1 mM naringenin were also performed with the same protocol to avoid confounding effects. Peak inward tail currents were measured to quantify relative blockade. Statistical analysis of results is summarised in Fig. 4d.

Human *ether-à-go-go*-related gene currents expressed in Xenopus oocytes exhibited a slow but continuous current increase under control conditions, i.e. during super-

Kinetics of onset and wash-out of the inhibitory effects

A standardised voltage protocol repeated at intervals of 15 s was used to monitor the kinetics of blockade and wash-out: voltage steps to +30 mV (400 ms) were applied, followed by a return pulse to −60 mV (400 ms) to evoke outward tail currents. The holding potential was −80 mV. Peak tail currents were measured to determine the degree of blockade. Single-exponential fits were used to obtain time constants of the time courses observed. The onset of blockade was fast with time constants of τ=1.47±0.24 min (n=5; Fig. 5a). Wash-out of naringenin-induced blockade was slower, but complete with τ=3.84±0.50 min (n=5; Fig. 5b).

Fig. 4 Functional significance of aromatic residues Tyr-652 and Phe-656 for binding of naringenin to HERG channels. The inhibitory effect of naringenin at a concentration of 1 mM was tested in **a** HERG wild type channels and in **b** HERG Y652A and **c** HERG F656A mutant channels. Results of n=5–6 experiments in each group are summarised in **d**. Potency of naringenin was markedly reduced in HERG F656A channels, but not in HERG Y652A channels. Protocol: holding potential −80 mV, first depolarising test pulse to +30 mV (400 ms), second repolarising pulse to −120 mV (400 ms). Peak tail currents were measured to quantify effects
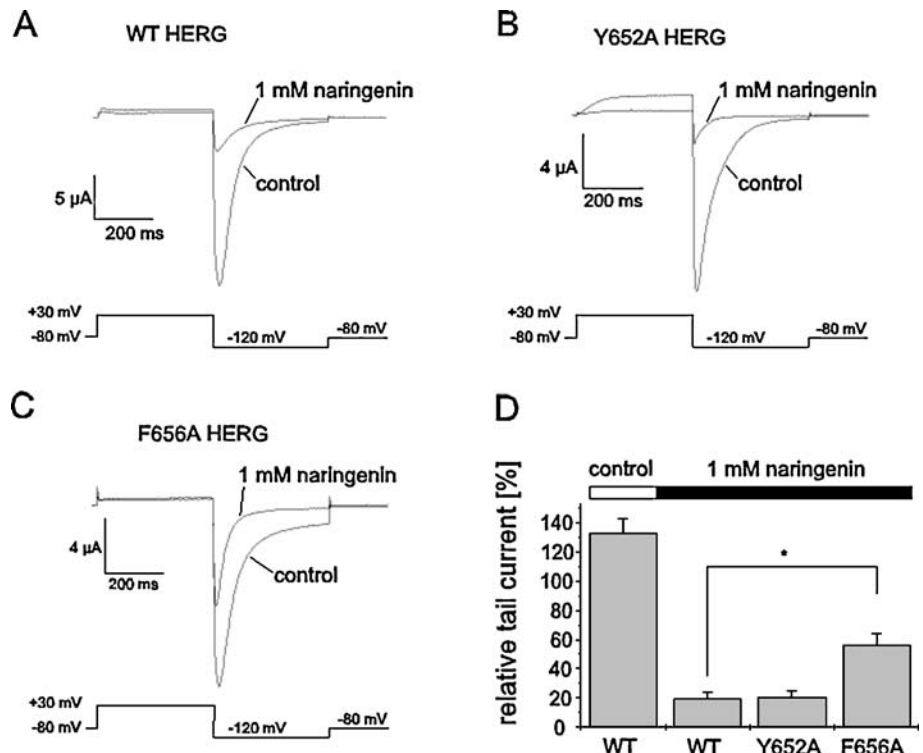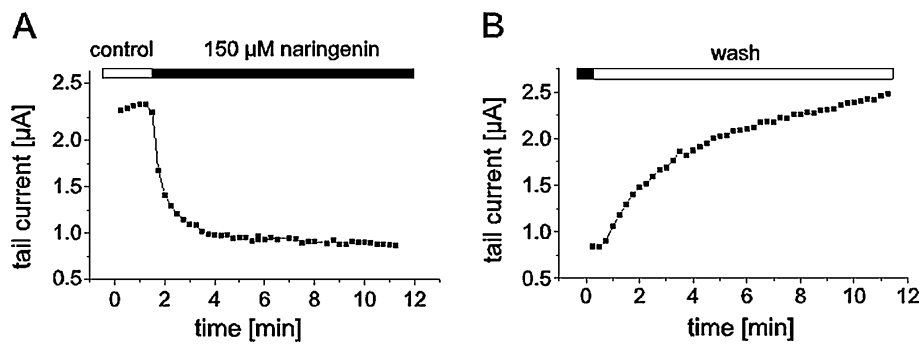
Fig. 5 Onset and wash-out of effects. To monitor onset and wash-out of blockade, 150 μM naringenin was **a** perfused into the bath and **b** washed out with the bath solution afterwards. Representative experiments are shown. Blockade was completely reversible upon wash-out. Protocol: repetitive pulsing at a frequency of 0.07 Hz, holding potential −80 mV, first pulse to +30 mV (400 ms), followed by a second pulse to −60 mV (400 ms)

Naringenin blocks HERG channels in the open and inactivated states

State dependence of blockade was examined with two different approaches. First, we tested whether naringenin binds to HERG channels in the open or closed states. Under control conditions, a long depolarising test pulse to 0 mV from a holding potential of −80 mV was applied, leading to activation of the channels (Fig. 6a). Then naringenin (150 μmol/l) was washed into the bath while holding the cell at −80 mV where HERG channels were in the closed state. After 10 min, the test pulse was repeated (Fig. 6a).
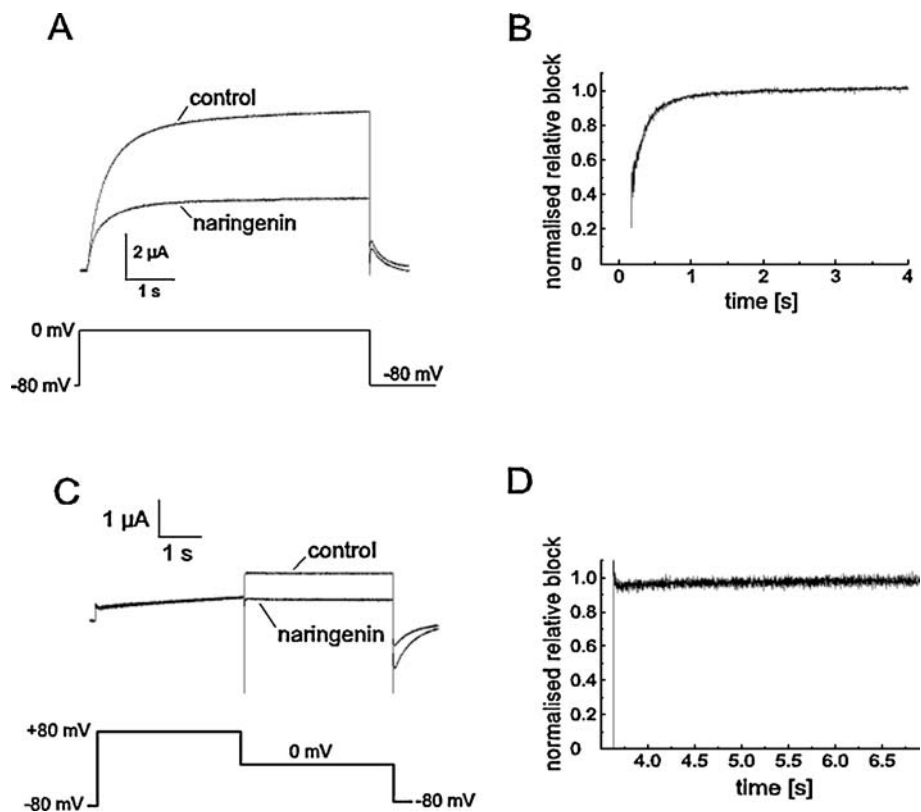

Fig. 6 State dependence of blockade. **a** Blockade of HERG channels in the open and closed states was studied with a one-step protocol activating the channels. Current traces recorded under control conditions and after incubation with naringenin (150 μM) are shown in superposition. **b** Time course of relative blockade calculated by division of these traces shows a rapid development of inhibition after opening of the channels in line with open channel blockade. **c** An inactivating step was added to the protocol to test whether HERG channels are also inhibited in the inactivated state. Again, measurements were recorded under control conditions and after incubation with naringenin (150 μM; superposition). **d** Time course of relative blockade calculated by division of these traces with the beginning of the second step as starting point is plotted. The inhibitory effect had already reached its maximum at the beginning of the second step. This points to a binding of naringenin to the channels in the preceding step, i.e. in the inactivated state. Protocol in **a**: holding potential −80 mV, long test pulse to 0 mV (3,500 ms). Protocol in **c**: holding potential −80 mV, first pulse to +80 mV (3,500 ms), second pulse to 0 mV (3,500 ms)

Relative blockade was calculated by division of the current traces under control conditions and after exposure to naringenin (Fig. 6b). The inhibitory effect developed fast after channel activation and may be estimated to start from 0. This points to a blockade of channels in the open state, but not in the closed state.

We then applied a two-step protocol to examine blockade of inactivated channels: a long first voltage step (3,500 ms) to +80 mV inactivated the channels, and a repolarising step to 0 mV induced recovery from inactivation resulting in an almost instantaneous outward current (Fig. 6c). Recordings and wash-in were performed as with the previous voltage protocol and relative blockade was calculated as described above. The inhibitory effect was found to be almost 100% at the starting point of channel activation by the second step (Fig. 6d). This result indicates development of blockade during the preceding step, i.e. in the inactivated state. Thus, naringenin probably binds to HERG channels in the open state and in the inactivated state, but not in the closed states.

Naringenin does not affect HERG current activation

We used the following test pulse protocol to investigate effects of naringenin on HERG current activation: from a holding potential of −80 mV, voltage steps to potentials ranging from −100 mV to +100 mV (400 ms) elicited activating currents and a return pulse to −120 mV (400 ms) evoked large inward tail currents. Measurements were recorded under control conditions (Fig. 7a) and after application of naringenin (150 μM) respectively (Fig. 7b). Peak tail currents were normalised and plotted as a function of the preceding test pulse potential to obtain HERG cur-

rent activation curves. Mean values and standard errors of $n=6$ experiments displayed in Fig. 7c show that naringenin did not affect HERG current activation.

Effects of naringenin on HERG current inactivation

Two different approaches were used to investigate effects on HERG current inactivation. First, we studied steady-state inactivation with the following protocol. Channels were inactivated at a holding potential of +20 mV. Short test pulses to potentials ranging from −120 mV to +10 mV (15 ms) in 10-mV increments were applied to recover the channels from inactivation. Returning to the holding potential of +20 mV after these test pulses evoked large outward inactivating currents. After recording a measurement under control conditions, the holding potential was set back to −80 mV during the wash-in period in order to avoid destruction of the oocyte, which occurs if it is clamped at +20 mV for several minutes. Typical recordings are shown in Fig. 8a (control) and Fig. 8b (after application of 150 μM naringenin). Outward current amplitudes measured 2 ms after the return to the holding potential were normalised, plotted as a function of the preceding test pulse potential and fitted with a Boltzmann function to obtain steady-state inactivation curves. In Fig. 8c mean data of $n=6$ experiments are shown. Naringenin induced a shift of the half-maximal inactivation voltage $V_{1/2}$ by 14.9 ± 3.7 mV to more negative potentials ($P=0.01$; $n=6$).

A different protocol was used to investigate the time course of inactivation. From a holding potential of −80 mV, a long test pulse to +40 mV (900 ms) served to inactivate the channels. Short pulses to −100 mV (16 ms) followed by voltage steps to potentials ranging from −60 mV to

Fig. 7 Naringenin does not affect HERG current activation. Representative current recordings **a** before and **b** after exposure to 150 μM naringenin, are shown. Peak tail currents were normalised and plotted as a function of the preceding test pulse potential to obtain HERG current activation curves (**c**; summary data of $n=6$ experiments). Naringenin did not affect HERG activation significantly. Protocol: holding potential −80 mV, first test pulse to potentials from −100 mV to +100 mV (400 ms), return pulse to −120 mV (400 ms)
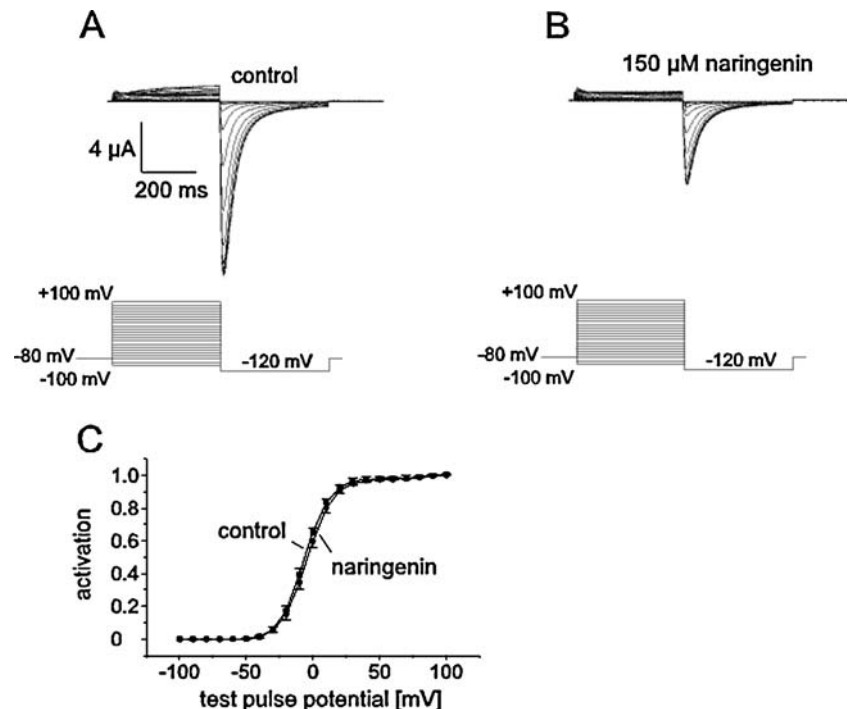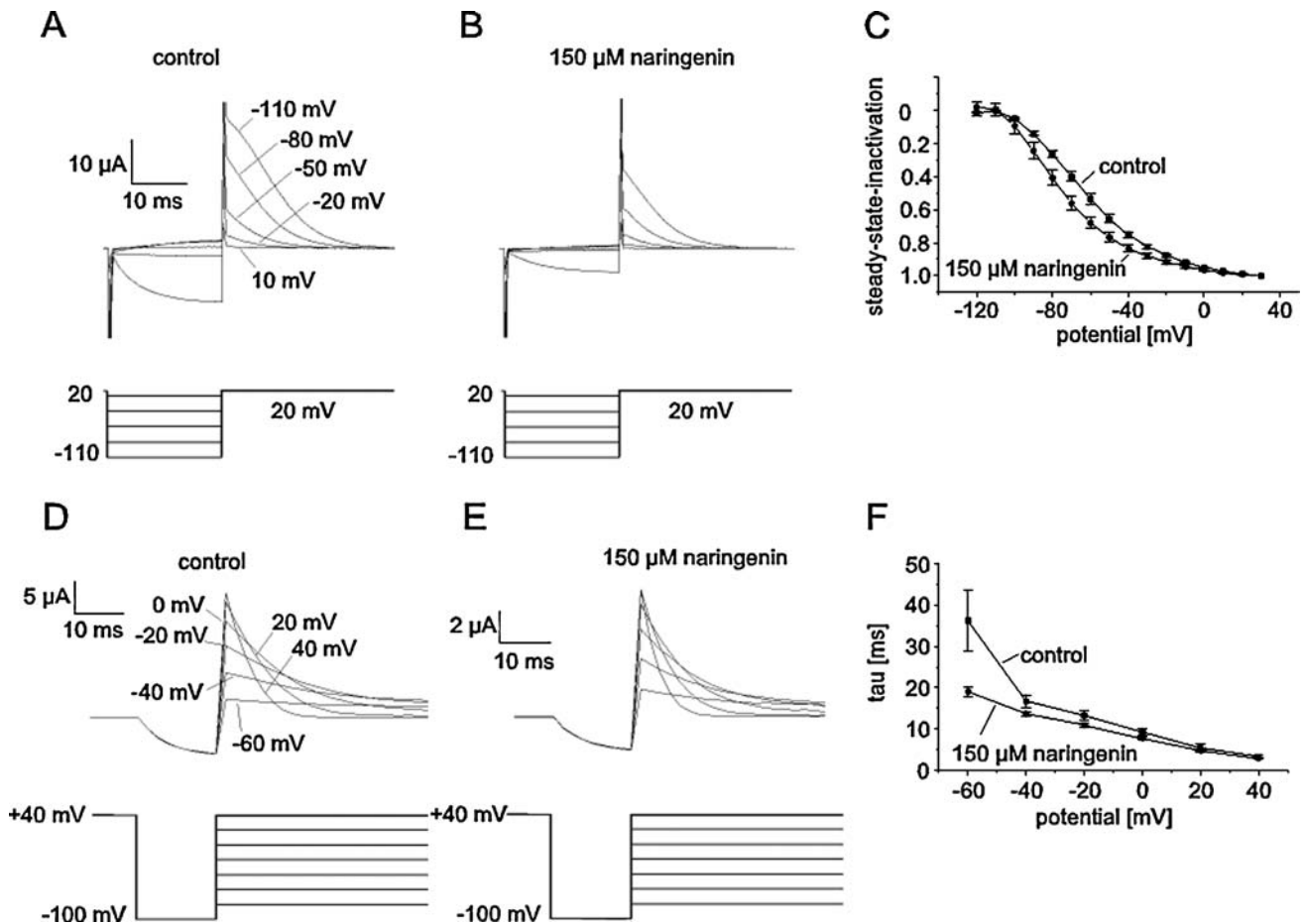
Fig. 8 Effects of naringenin on HERG current inactivation. First, HERG current steady-state inactivation was examined. Typical measurements **a** under control conditions and **b** after exposure to 150 μM naringenin are displayed. To improve the clarity of the figures, not all current traces are shown. **c** Outward inactivating currents 2 ms after the return to the holding potential were normalised, plotted as a function of the preceding test pulse potential and fitted with a Boltzmann function to obtain HERG current steady-state inactivation curves (summary data of *n*=6 experiments). Naringenin induced a shift of the half-maximal inactivation voltage by 14.9±3.7 mV to more negative potentials. Then the time course of HERG current inactivation was analysed. Representative current recordings **d** be-

fore and **e** after exposure to 150 μM naringenin are shown. Outward inactivating currents were fitted with single exponential functions to obtain time constants. **f** Time constants are plotted versus test pulse potential (summary data of *n*=6 experiments). Naringenin reduced time constants at −60 mV from 36.2±7.3 ms to 19.1±1.2 ms. Protocol in **a**, **b**: holding potential +20 mV, short test pulses to potentials ranging from −120 mV to +10 mV in 10-mV increments (15 ms), returning to +20 mV evoked large outward inactivating currents. Protocol in **d**, **e**: holding potential −80 mV, first test pulse to +40 mV (900 ms), second test pulse to −100 mV (16 ms), third test pulse to potentials ranging from −60 mV to +40 mV (150 ms) in 20-mV increments

+20 mV (150 ms) in 20-mV increments elicited large outward, inactivating currents. Currents under control conditions (Fig. 8d) and after incubation with 150 μM naringenin (Fig. 8e) were fitted with single exponential functions to obtain time constants. Summary data from *n*=6 experiments are plotted in Fig. 8f. Naringenin reduced time constants at −60 mV from 36.2±7.3 ms to 19.1±1.2 ms (*P*=0.04; *n*=6). Time constants at other potentials were not altered significantly.

Naringenin blockade is not frequency-dependent

Frequency-dependence of blockade was tested by repeating a short two-step voltage protocol at intervals of 1 s and 15 s. A first test pulse to 20 mV (300 ms) activated HERG

currents, and a second repolarising step to −40 mV (300 ms) elicited tail currents. The holding potential was −80 mV. Peak tail current amplitudes were measured to determine the degree of blockade.

Naringenin (150 μM) did not show significant differences in relative blockade measured at the two frequencies (*P*>0.05; *n*=6; Fig. 9).

Discussion

We have characterised the pharmacological properties of HERG blockade by naringenin in detail. To the best of our knowledge, this is the first study to investigate the electrophysiological features of a specific flavonoid.
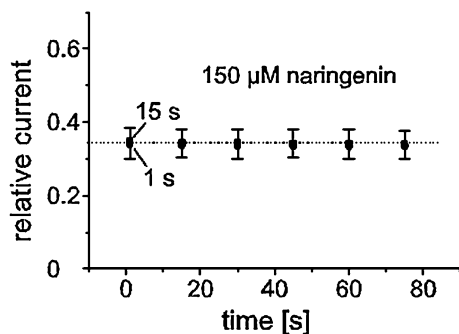
Fig. 9 Human *ether-à-go-go*-related gene blockade by naringenin is not frequency-dependent. In order to investigate frequency dependence, repetitive test pulses were applied at time intervals of 1 s and 15 s under control conditions and after exposure to naringenin. Peak tail currents were measured to determine relative blockade. Summary data of *n*=6 experiments at each frequency are shown. No significant difference was observed between the two frequencies. Protocol: from a holding potential of −80 mV, test pulses to +20 mV (300 ms) were applied to activate HERG currents, and tail currents were elicited by a second step to −40 mV (300 ms)

Naringenin concentrations in vitro and in vivo

Naringenin is a naturally occurring food compound that reaches concentrations of 150 µM in orange juice and even more than 1,000 µM in grapefruit juice (Ho and Saville 2001; Erlund et al. 2001). The corresponding glycoside naringin, which is metabolised to naringenin in the gut, is found in concentrations of over 2,000 µM in grapefruit juice (Ameer et al. 1996). In vivo studies detected maximum plasma naringenin levels of 6.0±5.4 µM 4–6 h after single oral ingestion of 8 ml/kg of grapefruit juice (Erlund et al. 2001).

In the *Xenopus* oocyte expression system, higher drug concentrations are needed to achieve effects on ion channels than in native cells (Redfern et al. 2003). This has been attributed to the follicular membranes of the oocytes and the yolk (Madeja et al. 1997). As a consequence, IC_{50} values obtained in *Xenopus* oocytes are generally about 3–30 times higher than the respective IC_{50} values in native cells (Madeja et al. 1997).

It is generally accepted that IC_{50} values determined in mammalian cell lines correlate well in in vivo experiments (Redfern et al. 2003). Thus, in order to allow reliable clinical conclusions, the IC_{50} value has to be measured in HEK cells in addition to *Xenopus* oocytes experiments (Redfern et al. 2003). In a previous study we therefore determined the potency of naringenin in HEK cells expressing HERG channels (Zitron et al. 2005): the IC_{50} value was 36.5 µM with an inhibitory effect of 13.8±2.4% that was still measurable at a concentration of 1 µM, i.e. well within the range of plasma concentrations documented in the literature.

Electrophysiological properties of HERG blockade by naringenin

Naringenin exhibited a fast onset of blockade and a complete reversibility of the inhibitory effect upon wash-out. From a pharmacological point of view these are favourable properties, as intended effects may be achieved quickly and are reversible. Naringenin induced a small shift of HERG current steady-state inactivation curves to more negative potentials. This is unlikely to have major influence on HERG-mediated currents in vivo. HERG channels were blocked in their open and inactivated states, but not in their closed states. Preferential open channel blockade is common among HERG inhibiting agents and has been associated with pore binding site Y652/F656 (Mitcheson et al. 2000; Scholz et al. 2003). We observed a reduced affinity of naringenin to HERG F656A channels, but not to HERG Y652A channels. Thus, Phe-656 appears to be functionally important for the binding of this compound to HERG, whereas Tyr-652 does not. It has been proposed that affinity to pore binding sites Tyr-652 and Phe-656 is associated with two principal structural characteristics: a hydrophobic feature, typically an aromatic group capable of engaging in pi-stacking with a Phe-656 side chain, and a basic nitrogen capable of undergoing a pi-cation interaction with Tyr-652 (Fernandez et al. 2004; Pearlstein et al. 2003). The chemical structure of naringenin (Fig. 1) contains aromatic groups, but lacks nitrogen atoms. This fits in well with our results indicating that Phe-656 is involved in the binding of naringenin to the channel, whereas Tyr-652 is not.

We did not observe a frequency dependence of the inhibitory effect of naringenin. However, clinical conclusions based on this result are limited by the fact that we used pulsing rates below the physiological range (corresponding to 60 bpm [1 Hz] and 4 bpm [0.07 Hz]).

Quick onset and wash-out of effects and lack of major electrophysiological modification of unblocked channels may be considered to be favourable features. The mode of action and the binding site of naringenin appear to be similar to those of well-characterised HERG blocking drugs (Redfern et al. 2003; Spector et al. 1996; Zitron et al. 2002; Numaguchi et al. 2000).

In this study, we have focussed on the effects of naringenin on HERG channels. In a review of the literature, we have not found any reports of the effects of naringenin on other ion channels. In view of a clinical judgement (Redfern et al. 2003; Karle et al. 2002), however, it will be both interesting and necessary to investigate these potential effects in further studies.

Proarrhythmic potential of naringenin

From a clinical point of view, HERG channel blockade has been associated with proarrhythmic effects, mainly the induction of torsade de pointes ventricular tachycardias, which may lead to sudden cardiac death (Redfern et al. 2003). Numerous compounds have been withdrawn from clinical use because of this side-effect and even more may only be used with specific precautions (Redfern et al. 2003).

Specific HERG channel blockers that were developed as pure class III antiarrhythmic agents such as dofetilide and

azimilide have been associated with a significant risk of proarrhythmia in clinical studies (Pratt 2003). Long-term treatment with these compounds did not lead to a survival benefit (Pratt 2003). The specific class III agent d-sotalol was even associated with increased mortality in the SWORD study (Waldo et al. 1996).

Dofetilide and azimilide exhibit IC_{50} values for HERG blockade in mammalian cells of 31.5 nM and 610 nM respectively (Jurkiewicz and Sanguinetti 1993; Walker et al. 2000). These values are within the therapeutic plasma concentrations (Redfern et al. 2003). The affinity of d-sotalol to HERG is rather low under in vitro conditions (Numaguchi et al. 2000). Due to the comparatively high daily doses, its good bioavailability, and its hydrophilic properties, however, it probably also causes significant $HERG/I_{Kr}$ blockade at therapeutic dosage (Redfern et al. 2003).

Naringenin has a low affinity to HERG in comparison to dofetilide and azimilide. The plasma concentrations reported in the literature are below the IC_{50} we have measured in HEK cells, which renders excessive QT prolongation unlikely. This is in line with our finding of a merely mild QTc prolongation (12.5 ms) even after ingestion of 1 l of grapefruit juice. However, there is a growing body of evidence demonstrating that patients who present with acquired long QT syndromes may have genetic risk factors (Priori and Napolitano 2002). This predisposition may be associated with a high susceptibility for proarrhythmic events induced by HERG antagonists.

Therefore, in view of clinical experience, ingestion of large amounts of naringenin should be avoided by patients at risk of torsade de pointes unless its safety can be proven in clinical studies. Particular caution is necessary in patients who have already presented with acquired long QT syndrome.

Potential antiarrhythmic effects of naringenin

Epidemiological studies have pointed out the preventive effects of flavonoids on cardiac mortality (Knekt et al. 1996; Hertog et al. 1993; Geleijnse et al. 2002; Yochum et al. 1999; Rimm et al. 1996; Mukamal et al. 2002). From a theoretical point of view, this could be a consequence of antiarrhythmic properties, e.g. the prevention of re-entry based arrhythmias in the context of myocardial ischemia by action potential prolongation (Huikuri et al. 1999; Singh and Nademanee 1985). However, as outlined in the previous paragraph, pure class III activity based on HERG channel blockade would not suffice to explain beneficial effects. Therefore, it is necessary to characterise additional electrophysiological effects of naringenin on cardiac electrophysiology and to study its proarrhythmic and antiarrhythmic properties in animal models.

Conclusions

In this study, we have demonstrated that the grapefruit flavonoid naringenin inhibits HERG channels with electrophysiological and biophysical properties in a similar way to well-characterised pharmaceutical HERG antagonists. These findings shed new light on the potential effects of dietary and phytotherapeutic compounds on cardiac electrophysiology. In view of potential proarrhythmic effects, patients at risk of torsade de pointes tachycardia should avoid ingestion of naringenin unless its safety can be proven in clinical studies. Electrophysiological effects of flavonoids deserve further investigation in animal studies and in epidemiological studies.

References

Ameer B, Weintraub RA, Johnson JV, Yost RA, Rouseff RL (1996) Flavanone absorption after naringin, hesperidin, and citrus administration. Clin Pharmacol Ther 60:34–40

Curran ME, Splawski I, Timothy KW, Vincent GM, Green ED, Keating MT (1995) A molecular basis for cardiac arrhythmia: HERG mutations cause long QT-syndrome. Cell 80:795–803

De Lorgeril M (1998) Mediterranean diet in the prevention of coronary heart disease. Nutrition 14:55–57

Erlund I, Meririnne E, Alfthan G, Aro A (2001) Plasma kinetics and urinary excretion of the flavanones naringenin and hesperetin in humans after ingestion of orange juice and grapefruit juice. J Nutr 131:235–241

Fernandez D, Ghanta A, Kauffman G, Sanguinetti M (2004) Physical chemical features of the HERG channel drug binding site. J Biol Chem 279:10120–10127

Geleijnse JM, Launer LJ, Van der Kuip DAM, Hofmann A, Wittemann JCM (2002) Inverse association of tea and flavonoid intakes with incident myocardial infarction: the Rotterdam study. Am J Clin Nutr 75:880–886

Hertog MG, Feskens EJ, Hollman PC, Katan MB, Kromhout D (1993) Dietary antioxidant flavonoids and risk of coronary heart disease: the Zutphen elderly study. Lancet 342:1007–1011

Ho P, Saville DJ (2001) Inhibition of human CYP3A4 activity by grapefruit flavonoids, furanocoumarins and related compounds. J Pharm Pharmaceut Sci 4:217–227

Huikuri HV, Castellanos A, Myerburg RJ (1999) Sudden death due to cardiac arrhythmias. N Engl J Med 345:1473–1482

Jurkiewicz NK, Sanguinetti MC (1993) Rate-dependent prolongation of cardiac action potentials by a methanesulfonanilide class III antiarrhythmic agent. Specific block of rapidly activating delayed rectifier K+ current by dofetilide. Circ Res 72:75–83

Karle C, Thomas D, Kiehn J (2002) The antiarrhythmic drug BRL-32872. Cardiovasc Drug Rev 20:111–120

Kiesecker C, Zitron E, Lück S, Bloehs R, Scholz EP, Kathöfer S, Thomas D, Kreye VA, Katus HA, Schoels W, Karle CA, Kiehn J (2004) Class Ia antiarrhythmic drug ajmaline blocks HERG potassium channels: mode of action. Naunyn-Schmiedebergs Arch Pharmacol 417:221–228

Knekt P, Jarvinen R, Reunanen A, Maatela J (1996) Flavonoid intake and coronary mortality in Finland: a cohort study. Brit Med J 312:478–481

Madeja M, Musshoff U, Speckmann EJ (1997) Follicular tissues reduce drug effects on ion channels in oocytes of *Xenopus laevis*. Eur J Neurosci 9:599–604

Middleton E Jr, Kandaswami C, Theoharides TC (2000) The effects of plant flavonoids on mammalian cells: implications for inflammation, heart disease, and cancer. Pharmacol Rev 52:673–751

Mitcheson JS, Chen J, Lin M, Culberson C, Sanguinetti MC (2000) A structural basis for drug-induced long QT syndrome. Proc Natl Acad Sci U S A 97:12329–12333

Mukamal KJ, Maclure M, Muller JE, Sherwood JB, Mittleman MA (2002) Tea consumption and mortality after acute myocardial infarction. Circulation 105:2476–2481

Numaguchi H, Mullins FM, Johnson JP, Johns DC, Po SS, Yang IC, Tomaselli GF, Balser JR (2000) Probing the interaction between inactivation gating and d-sotalol block of HERG. Circ Res 87:1012–1018

Pearlstein RA, Vaz RJ, Kang J, Chen XL, Preobrazhenskaya M, Shchekotikhin AE, Korolev AM, Lysenkova LN, Miroshnikova OV, Hendrix J, Rampe D (2003) Characterization of HERG potassium channel inhibition using CoMSiA 3D QSAR and homology modelling approaches. Bioorg Med Chem Lett 13:1829–1835

Pratt CM (2003) Pure class III agents for prevention of sudden cardiac death. J Cardiovasc Electrophysiol 14 [Suppl]:S82–S86

Priori SG, Napolitano C (2002) Genetic defects of cardiac ion channels. The hidden substrate for torsade de pointes. Cardiovasc Drugs Ther 16:89–92

Redfern WS, Carlsson L, Davis AS, Lynch WG, MacKenzie I, Palethorpe S, Siegl PK, Strang I, Sullivan AT, Wallis R, Camm AJ, Hammond TG (2003) Relationships between preclinical cardiac electrophysiology, clinical QT interval prolongation and torsade de pointes for a broad range of drugs: evidence for a provisional safety margin in drug development. Cardiovasc Res 58:32–45

Renaud S, de Lorgeril M (1992) Wine, alcohol, platelets, and the French paradox for coronary heart disease. Lancet 339:1523–1526

Rimm EB, Katan MB, Ascheiro A, Stampfer MJ, Willet WC (1996) Relation between intake of flavonoids and risk for coronary heart disease in male health professionals. Ann Intern Med 125:384–389

Scholz EP, Zitron E, Kiesecker C, Lueck S, Kathöfer S, Thomas D, Weretka S, Peth S, Kreye VA, Schoels W, Katus HA, Kiehn J, Karle CA (2003) Drug binding to aromatic residues in the HERG channel pore cavity as possible explanation for acquired long QT syndrome by antiparkinsonian drug budipine. Naunyn-Schmiedebergs Arch Pharmacol 368:404–414

Singh BN, Nademanee K (1985) Control of cardiac arrhythmias by selective lengthening of repolarisation: theoretic considerations and clinical observations. Am Heart J 109:421–430

Spector PS, Curran ME, Keating MT, Sanguinetti MC (1996) Class III antiarrhythmic drugs block HERG, a human cardiac delayed rectifier K^+ channel. Circ Res 78:499–503

Waldo AL, Camm AJ, de Ruyter H, Friedman PL, MacNeil DJ, Pauls JF, Pitt B, Pratt CM, Schwartz PJ, Veltri EP (1996) Effect of D-Sotalol on mortality in patients with left ventricular dysfunction after recent and remote myocardial infarction. The SWORD investigators. Survival with Oral D-Sotalol. Lancet 348:7–12

Walker BD, Singleton CB, Tie H, Bursill JA, Wyse KR, Valenzuela SM, Breit SN, Campbell TJ (2000) Comparative effects of azimilide and ambasilide on the human-ether-a-gogo-related gene (HERG) potassium channel. Cardiovasc Res 48:44–58

Witchel HJ, Milnes JT, Mitcheson JS, Hancox JC (2002) Troubleshooting problems with in vitro screening of drugs for QT interval prolongation using HERG K^+ channels expressed in mammalian cell lines and Xenopus oocytes. J Pharmacol Toxicol Methods 48:65–80

Yochum L, Kushi LH, Meyer K, Folsom AR (1999) Dietary flavonoid intake and risk of cardiovascular disease in postmenopausal women. Am J Epidemiol 149:943–949

Zitron E, Karle CA, Wendt-Nordahl G, Kathofer S, Zhang W, Thomas D, Weretka S, Kiehn J (2002) Bertosamil blocks HERG potassium channels in their open and inactivated states. Br J Pharmacol 137:221–228

Zitron E, Scholz EP, Owen R, Lück S, Kiesecker C, Thomas D, Kathöfer S, Niroomand F, Kiehn J, Kreye VA, Katus HA, Schoels W, Karle CA (2005) QTc prolongation by grapefruit juice and its potential pharmacologic basis: HERG channel blockade by flavonoids. Circulation 111:835–838